In situ observations on the austenite stability in TRIP-steel during tensile testing

Suzelotte Kruijver, Lie Zhao, Jilt Sietsma, Erik Offerman, Niels van Dijk, Lawrence Margulies, Erik Lauridsen, Stephan Grigull, Henning Poulsen, and Sybrand van der Zwaag

In-situ deformation tests have been performed on a steel displaying the transformation-induced plasticity (TRIP) effect, while monitoring the phase transformation by means of X-ray diffraction. A tensile stress is applied to 0.4 mm thick samples of this steel with mass contents of 0.26 % Si, 1.5 % Mn, and 1.8 % Al in a transmission geometry for a synchrotron-radiation beam of 25 μm · 25 μm. On the diffraction patterns every grain appears as a discrete spot The austenite {200} reflections are analysed during this investigation.
The diffraction patterns are treated like a powder pattern for five different η-angles, with η representing the angle between the tensile direction and the normal direction of the diffracting {200} planes. The results of the analysis show that $\eta = 0°$ and $\eta = 90°$ are the preferential orientations for the transformation to martensite. The Ludwigson and Burger model [9] is used to gain more information about the stress dependence of the deformation induced martensite formation. The microdiffraction patterns also reveal the changes in carbon concentration in austenite at each retained austenite fraction.

Aims and scope

Transformation induced plasticity steels show excellent mechanical properties. These properties mainly arise from a martensitic transformation of the metastable retained austenite induced by stress. For the development of TRIP steels knowledge of the mechanical stability of the retained austenite is of crucial importance. The stability of austenite is determined by, in an as yet unspecified manner; the chemical composition (especially the carbon content), grain size, temperature and the orientation of the grain with respect to the stress field [1...3].

The retained austenite is the result of a dedicated heat treatment during steel production. A common heat treatment for TRIP steel is an intercritical anneal followed by austempering at the bainite forming temperature. During the heat treatment the austenite phase is stabilised by enrichment in carbon.

The carbon concentration depends on the process conditions. It is unlikely that all austenite grains have the same carbon concentration, due to fluctuations in the process and the immediate surroundings of the grains. A distribution of the carbon concentration over the grains is therefore expected to exist [4].

It would be highly desirable to follow the disappearance of individual retained austenite grains as a function of applied stress and carbon concentration of the grain. The 3D X-ray diffraction microscope at beamline ID11 of the European Synchrotron Radiation Facility equipped with a stress-rig gives the opportunity to follow the development of individual grains [5; 6].

Every individual austenite grain gives a spot on the diffraction pattern, which disappears when the austenite grain transforms to martensite. By characterisation of the austenite spots as a function of deformation it is possible to find the stress, strain and microstructural conditions under which the transformation of the austenite takes place.

Characteristics of a diffraction spot are the 2θ-position, the η-position and the intensity. The definition of the 2θ-position and the η-position are shown in **figure 1**. The carbon content of the grain and the local stress condition determine the 2θ-peak position of the spot. The η-peak position reveals the orientation of the grain with respect to the applied stress. The intensity of the spot depends on the grain size.

During this investigation the diffraction pattern characterising of the retained austenite while increasing the strain

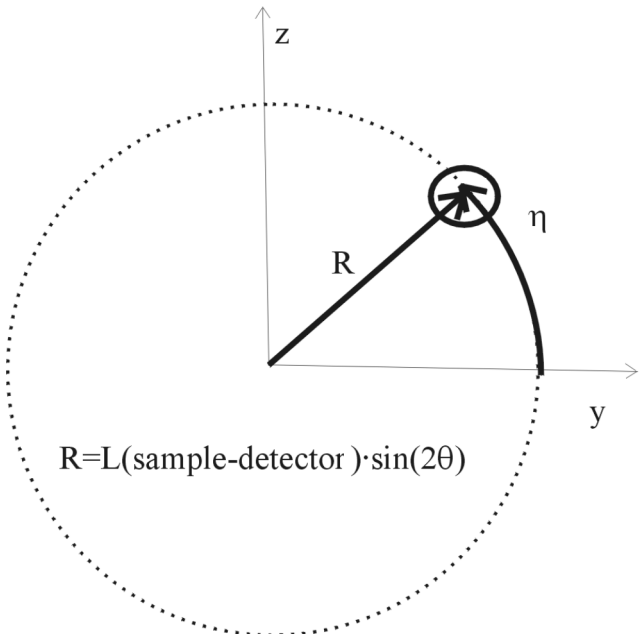

Figure 1. The definition of 2θ-position and the η-angle in a diffraction pattern

Ir. Suzelotte Kruijver, PhD. researcher; *Dr. Lie Zhao,* Post-doc researcher, Netherlands Institute for Metals Research, Delft*; Dr. Jilt Sietsma*, associate professor, Materials Science and Technology; *ir. Erik Offerman,* PhD. researcher, Interfaculty Reactor Institute and Materials Science and Technology; *Dr. ir. Niels van Dijk*, researcher, Interfaculty Reactor Institute, Delft University of Technology, The Netherlands*; Dr. Lawrence Margulies,* senior scientist, European Synchrotron Radiation Facility, France, and Materials Research Department, Risø National Laboratory, Denmark*; Dr. Erik Lauridsen,* post-doc researcher, Materials Research Department, Risø National Laboratory, Denmark; *Dr Stephan Grigull,* beamline scientist, European Synchrotron Radiation Facility, France; *Dr. Henning Poulsen,* senior scientist, Materials Research Department, Risø National Laboratory, Denmark*; Prof. dr. ir. Sybrand van der Zwaag,* professor, Materials Science and Technology, Delft University of Technology, and NIMR Netherlands Institute for Metals Research, Delft, The Netherlands.

level up to 12 % is determined. The stability of the retained austenite is studied as a function of the orientation of the grains and the stress level. Moreover, the development of the carbon concentration is investigated.

Experimental procedure

The chemical composition of the used material, which is an experimentally produced grade, is given in **table 1**. The material was hot-rolled to a thickness of 2 mm. The casting and rolling were performed by the group of Prof. Dr.-Ing. R. Kawalla of the Institut für Metallformung of the Technischen Universität Bergakademie Freiberg.

Table 1. Chemical composition of the used material

Elements	C	Si	Mn	Al	Fe
mass contents in %	0.17	0.26	1.5	1.8	rest

The tensile sample was shaped by milling and thinned by grinding to a thickness of 0.4 mm. A diagram of the tensile sample used is shown in **figure 2**, where the rolling direction of the material is indicated.

After machining, the material was heat-treated in two salt baths. The heat treatment was first an intercritical anneal at 900 °C for 10 min. It was then immediately quenched to a salt bath of 400 °C for 2 min to form bainite and stabilise the austenite, and subsequently it was water-quenched.

This heat treatment gives a multiphase material, containing 10 % of austenite, with a carbon content of 1.7 % and the rest ferrite, martensite and bainite, obtained for a separate sample with the same heat treatment by normal X-ray diffraction. The average grain size of the austenite grains is about 1 μm [7].

The experimental setup is shown in **figure 3**. Note that the tensile direction is in the rolling direction of the material. The tensile extension was carried out using an Instron 25 kN stress-rig to deform to various strain levels of up to 12 %. The strain levels at which diffraction patterns were recorded are: 0, 0.5, 1, 1.5, 2, 3, 4, 5, 6, 8, 10 and 12 %.

The stress-rig extended the sample from one strain level to the next strain level in one minute. This makes the maximum strain rate about $3 \cdot 10^{-4}$ s^{-1}. The strain level was controlled during the experiments. At each strain level the sample was held for about 30 min to collect the diffraction patterns.

For the microdiffraction experiments a beam size of 25 μm · 25 μm was used and a wavelength of 0.0155 nm. The measurements are performed in transmission geometry. The diffraction patterns were detected by a CCD detector and were taken with an exposure time of 30 s and an oscillation angle in ω of 0.5°.

Results

An example of a diffraction pattern is given in **figure 4**. The different {hkl}-reflections of austenite and ferrite are indicated in the image. The austenite {200} reflection, at 2 $\theta \cong 4.9$ are analysed and presented in this paper.

In the present analysis the individual austenite spots are not distinguished, but the diffraction patterns are treated like powder patterns. The reflections are averaged over ±10° around a given η-angle. By doing this analysis for several η-angles the influence of the orientation on the relation between stability and stress is revealed. The analysis will be extended and refined in the near future.

The thermal noise of the camera (the darkcurrent and read-out noise) is subtracted by using a darkfield image with the same exposure time as used for the diffraction patterns. A darkfield image is an image taken without exposing the camera to any X-rays.

After this noise correction the data is normalised for the intensity of the beam, because the intensity of the beam changes during the measurements.

For the analysis of the data the program FIT2D is used [10]. An example of the results of FIT2D is given in **figure 5**. The program gives the intensity per area from the centre to the edge of the diffraction pattern in 654 radial

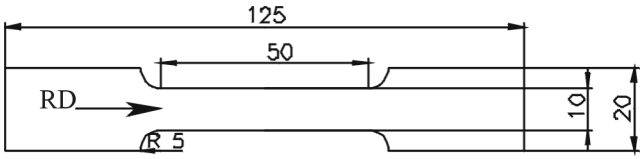

Figure 2. Sketch of a tensile sample. All dimensions are in millimeters

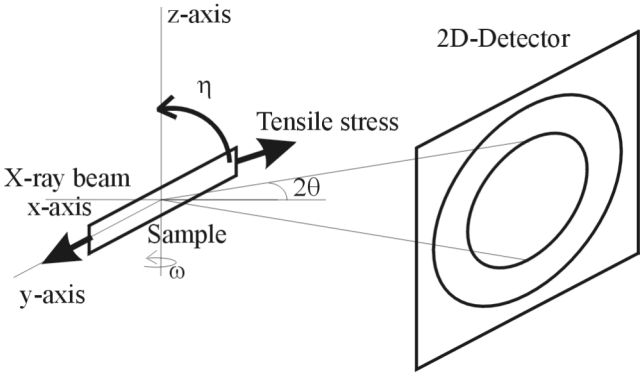

Figure 3. Experimental setup

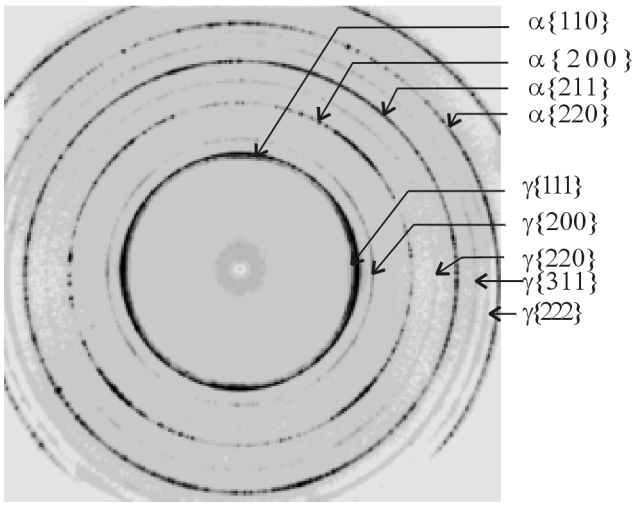

Figure 4. Example of a diffraction pattern

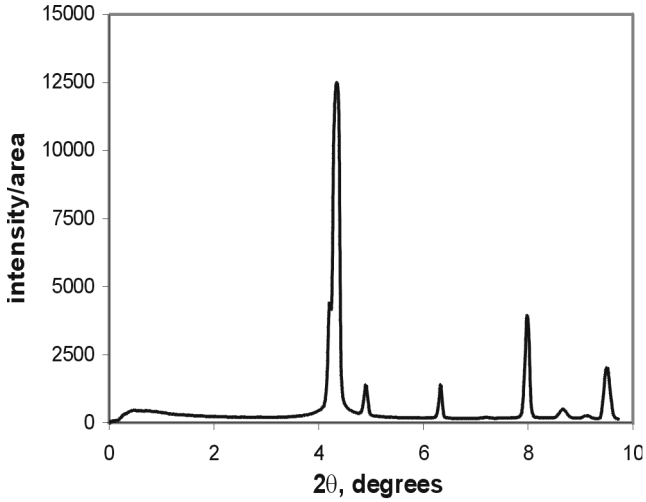

Figure 5. Example of a result of FIT2D, for $\eta_I = 0°$ and $\varepsilon = 0$ %

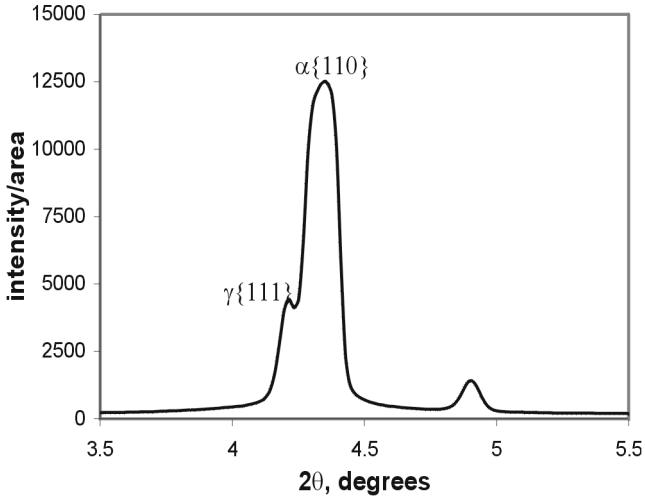

Figure 6. Austenite {200} peak on the tail of the ferrite {110} peak, for $\eta_I = 0°$ and $\varepsilon = 0$ %

bins, covering η_i-10° < η < η_i +10° for η_i = 0°, 30°, 45°, 60° and 90°. The radial bins are recalculated to degrees by Bragg's law using the position of the austenite reflection using Co$K\alpha$ radiation in a normal X-ray experiment on a separate sample of the same material.

The {200} austenite reflections are on the tail of the {110} ferrite reflections, an example of which is shown in **figure 6**. The ferrite tail is fitted by a polynomial equation and subtracted from the data. This yields a good fit of the background except for the dark current, which has already been subtracted.

The remaining {200} austenite peak is fitted by a Gaussian peak. This fit gives the peak intensity and the peak position. The peak intensity is linear with the austenite fraction. The fraction austenite versus stress is shown in **figure 7**. The graph shows that the fraction austenite decreases with increasing stress. At the maximum stress, which is at 12 % strain and is not the fracture stress, there is still about 4 % austenite left. The grains with the $\eta = 0°$ or $\eta = 90°$ orientation transform preferentially. The difference between these two orientations is not significant.

The stress effect and the carbon content of the austenite grains determine the peak position. An equation is derived for the peak shift due to stress. The stress is applied along the y-direction, the X-ray beam along the x-axis and the z-axis is vertical (figure 3). Austenite is a cubic crystal. The cube axes of the crystal are taken along the $x_c y_c z_c$-system. The $x_c y_c z_c$-system is rotated over an angle η around the x-axis with respect to the $x_c y_c z_c$ -system. The peak shift due to stress is caused by the strain ε_2 in the y_c-direction. This strain can be written as:

$$\varepsilon_2 = \frac{(c_{11}+c_{12})\cos^2\eta - c_{12}\sin^2\eta}{(c_{11}+2c_{12})(c_{11}-c_{12})}\cdot\sigma \,. \qquad (1)$$

The ratio $\dfrac{\varepsilon_2(\eta=90°)}{\varepsilon_2(\eta=0°)}$ is $-\dfrac{c_{12}}{c_{11}+c_{12}}$, which equals the Poisson ratio (ν = 0.4). The equation is fitted to the first two measuring points assuming that at low strains the stress effect is the dominant factor of the peak shift, since for all η-angles no significant transformation, and consequently no carbon enrichment, has yet occurred at σ = 412 MPa.

The fit gives the values for c_{11} and c_{12}, where c_{11} = 217 GPa and c_{12} = 145 GPa. **Figure 8** shows the peak shift caused by the stress and the measured data points. For η = 60° and η = 90° the peak shift caused by stress leads to an expansion and the other angles a contraction.

After subtracting the stress effect from the peak position, the remaining peak shift is due to the change in the effect of the carbon content of the remaining austenite. From this peak shift it is possible to reveal the carbon concentration by assuming the following relation between the carbon concentration x_c and the austenite lattice parameter a:

$$a = a_0 + \mu x_c \qquad (2)$$

where μ = 0.00467 nm/% [4] and a_0 is the lattice parameter at x_c = 0.

Using this equation the carbon concentration can be calculated from every peak position. The carbon concentra-

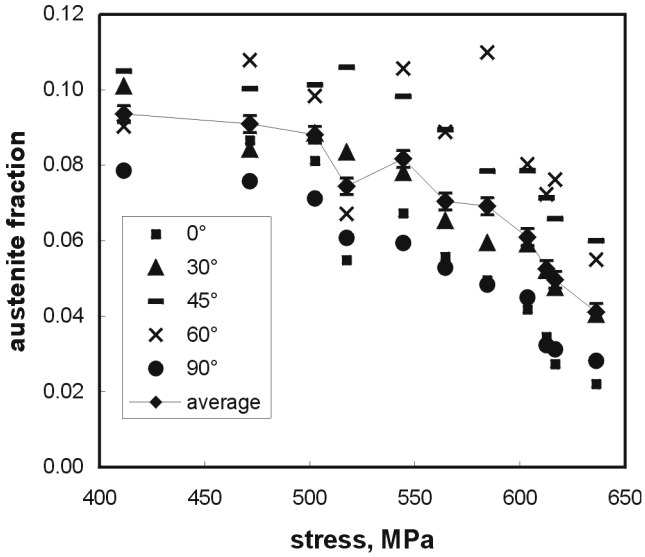

Figure 7. Austenite fraction vs. stress for indicated values of η_i

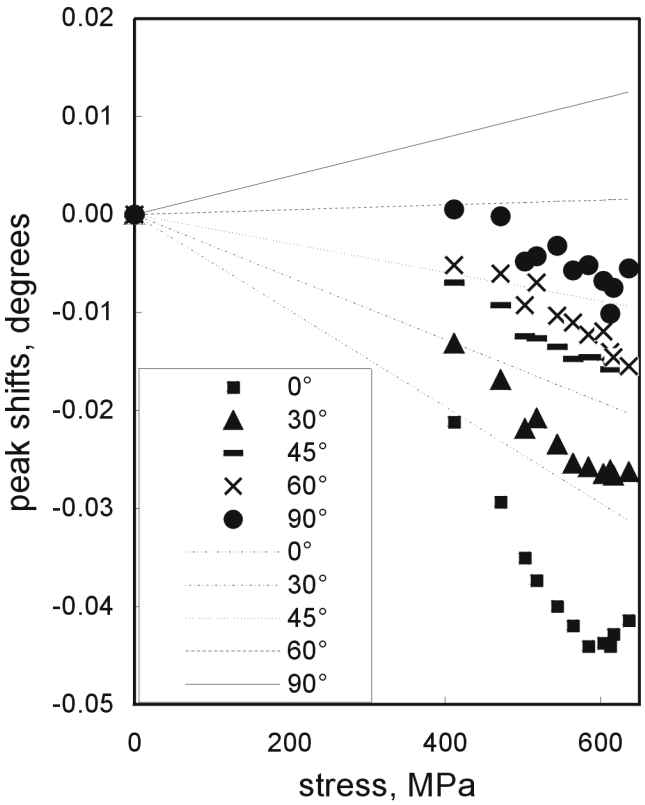

Figure 8. The calculated peak shift caused by stress (straight lines) and the measured data points for indicated values of η_I

tion versus fraction retained austenite is shown in **figure 9**. There is a significant trend that the carbon concentration increases for decreasing austenite fraction, in line with an expected increase in retained austenite stability with increasing carbon concentration [2].

Discussion

The stability of retained austenite was also investigated by Itami et al [8] and Girault et al [9]. Itami used a 1.9 % Si – 1.7 % Mn TRIP steel and X-ray diffraction Mo$K\alpha$ radiation for his investigation. Girault et al. tested two alloys, 1.5 % Si - 1.5 % Mn and a 1.5 % Al - 1.5 % Mn TRIP steel. Girault et al. measured the retained austenite by X-ray diffraction using Cu$K\alpha$ radiation. Results of their measurements are plotted in **figure 10** together with the average of the results of this investigation. The retained austenite fraction is plotted against the strain level. The trend of the result of this investigation is similar to the results of the other investigations, only Itami et al. started with a higher retained austenite fraction.

To quantify the kinetics of the deformation-induced martensite transformation as a function of strain, the Ludwigson and Burger relation [8] is used. The expression is:

$$\frac{1}{V_\gamma} - \frac{1}{V_{\gamma 0}} = \left(\frac{k_p}{p}\right)\varepsilon^p \qquad (3)$$

where V_γ is the volume fraction of austenite, $V_{\gamma 0}$ is the initial austenite fraction, k_p is a constant relating to the stability of retained austenite with respect to deformation, and p is the strain exponent of the autocatalytic effect. The exponent p can be assumed to be 1 for TRIP steels. The higher the k_p-value, the less stable is the retained austenite.

The Ludwigson and Burger equation is used to fit the four data sets. The fits are shown in **figure 11**. The k_p-values for the different materials are shown in **table 2**. It can be seen that the material used for this investigation has a similar stability to the material used by Girault et al [9]. The material used by Itami et al. [8] is less stable.

The advantage of using the 3D X-ray diffraction microscope instead of the normal X-ray diffraction is that it is

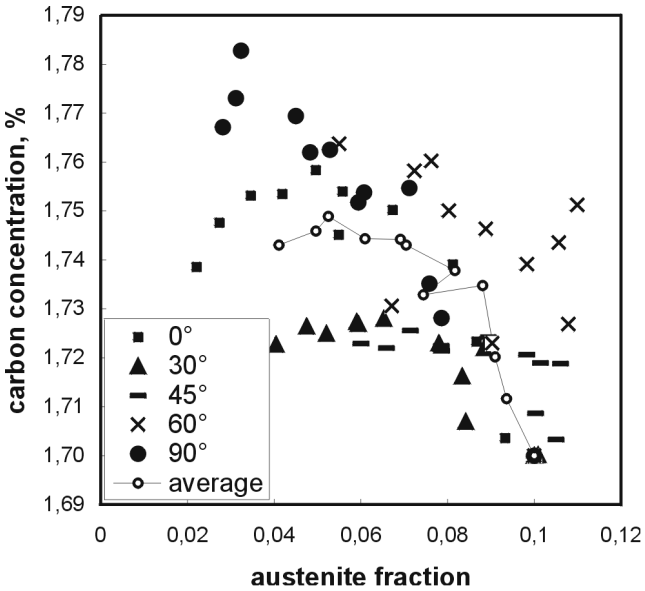

Figure 9. Carbon concentration vs. fraction for indicated values of η_I

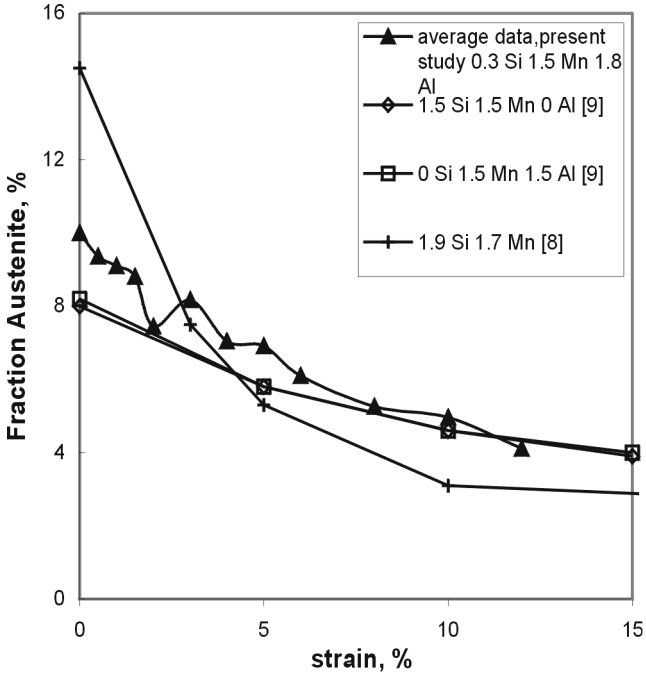

Figure 10. Retained austenite fraction vs. strain. The results shown are from Itami et al. [8], Girault et al. [9] and the average of the experimental data

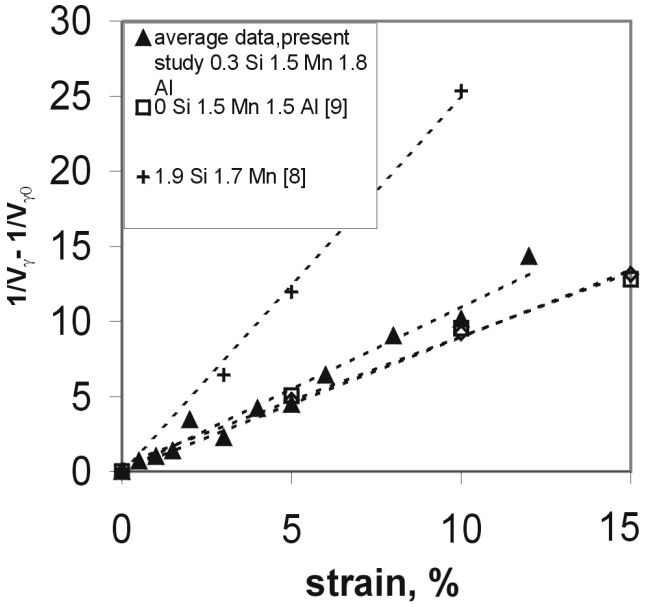

Figure 11. Fit of the Ludwigson and Burger relation to the data of Itami et al. [8], Girault et al. [9] and the average of the experimental data in the present study

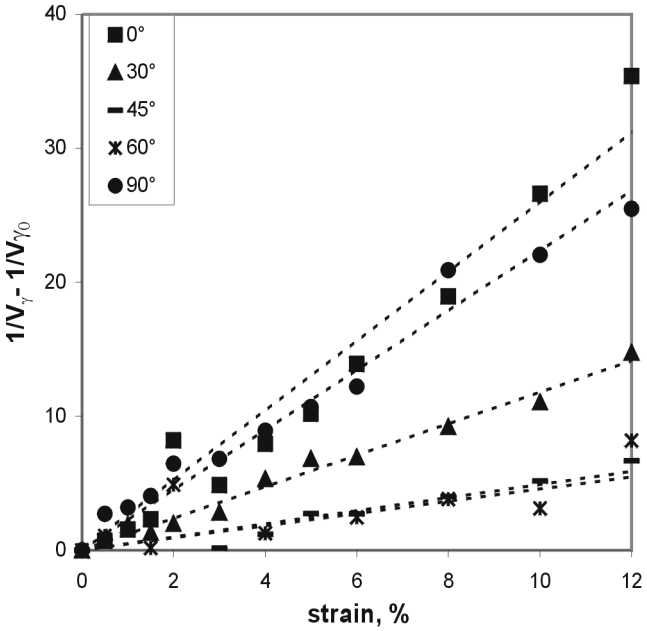

Figure 12. Fit of the Ludwigson Burger relationship to the data points for different η_l-angles

Table 2. k_p -values for the different materials

Material	average	1.5 % Si 1.5 % Mn [8]	1.5 % Mn 1.5 % Al [8]	1.9 % Si 1.7 % Mn [9]
k_p	110	90	90	248

Table 3. k_p -values for the different η -orientations

η-angle	0°	30°	45°	60°	90°	average
k_p	260	120	49	47	220	110

possible to reveal the effect of orientation of the crystal with respect to the applied stress on the transformation.

Results of the fit of the Ludwigson and Burger relationship on the data for the different η-angles are shown in **figure 12.** The relationship fits the data well. The k_p -values for the different η-angles are shown in **table 3**. The results of the fit show, analogous to figure 7, that η = 0° and η = 90° are the preferential orientations of the transformation to martensite. Results of Oliver et al. [3] also showed these preferential orientations for a steel with Ni mass contents of 25 % and C mass contents of 0.4 %.

Conclusions

The 3D X-ray diffraction microscope gives unique information on the carbon concentration of the retained austenite and the austenite fraction at each strain level for several orientations.

The used material has a mechanical stability comparable with materials from literature.

The η = 0° and η = 90° are the preferential orientations for the transformation to martensite.

It is possible to determine the change in carbon concentration in austenite as a function of the remaining retained austenite. A more extensive and detailed analysis of the data will be reported elsewhere.

Acknowledgements

The authors like to thank the European Synchrotron Radiation facility for providing the measuring time at ID-11.

References

[1] *Raghavan, V.:* Kinetics of martensitic transformation: Martensite a tribute to Morris Cohen, ASM Intern. (1992), p. 197/225.

[2] *Zhao, L.; Tegus, O.; Brück, E.; van Dijk, N. H.; Kruijver, S.; Sietsma, J.; van der Zwaag, S.*: Magnetic determination of thermal stability of retained austenite in TRIP steel, [in:] Proc. Intern. Conf. on TRIP-Aided High Strength Ferrous Alloys, Ghent, 19.-21. June 2002, p. 71/74.

[3] *Oliver, E. C.; Withers, P. J.; Daymond, M. R.; Ueta, S.; Mori, T.:* Neutron Diffraction Study of Stress Induced Martensitic Transformation in TRIP steel, Appl. Phys. A, to be published.

[4] *De Meyer, M.; Vanderschueren, D.; De Blauwe, K.; De Cooman, B. C.:* The Characterization of Retained Austenite in TRIP steels by X Ray Diffraction, [in:] 41st MWSP Conf. Proc., ISS, 1999, vol. 37, p. 483/91.

[5] *Juul Jensen, D.; et al.:* Plastic deformation and recrystallization studied by the 3D X-ray microscope, 1999 MRS Fall Meeting Symp. R Applications of synchrotron radiation techniques to materials science V, Nov. 29th - Dec. 3rd, 1999, Boston, p. 227/240.

[6] *Margulies, L.; Winther, G.; Poulsen, H.F.:* Science 291, p. 2392/94.

[7] *Zhao, L.; Dijk, N. H. van:* in preparation.

[8] *Itami, A.; Takahashi, M.; Usihioda, K.:* ISIJ Intern. 35 (1995) No. 9, p. 1121/27.

[9] *Girault, E.; Mertens, A.; Jacques, P.; Houbaert, Y.; Verlinden, B.; Van Humbeeck, J.:* Scripta mater. 44 (2001), p. 885/92.

[10] *Hammersly, A.P.; Riekel, C.:* High Press. Res. 14 (1996), p. 235/48.